HHS Public Access

Author manuscript

J Thromb Haemost. Author manuscript; available in PMC 2021 November 01.

Published in final edited form as:

J Thromb Haemost. 2020 November ; 18(11): 2899–2909. doi:10.1111/jth.15037.

Model-dependent contributions of FXII and FXI to venous thrombosis in mice

Steven P Grover[*], **Tatianna M Olson**[*], **Brian C Cooley**[†], **Nigel Mackman**[*]

[*] UNC Blood Research Center, Division of Hematology and Oncology, Department of Medicine, University of North Carolina at Chapel Hill, Chapel Hill, North Carolina, USA.

[†] McAllister Heart Institute, Department of Pathology and Laboratory Medicine, University of North Carolina at Chapel Hill, Chapel Hill, NC, USA.

Abstract

Background—The intrinsic pathway factors (F) XII and FXI have been shown to contribute to thrombosis in animal models. We assessed the role of FXII and FXI in venous thrombosis in three distinct mouse models.

Methods—Venous thrombosis was assessed in mice genetically deficient for either FXII or FXI. Three models were used: the inferior vena cava (IVC) stasis, IVC stenosis and femoral vein electrolytic injury models.

Results—In the IVC stasis model, FXII and FXI did not affect the size of thrombi but their absence was associated with decreased levels of fibrin(ogen) and an increased levels of the neutrophil extracellular trap (NET) marker citrullinated histone H3. In contrast, a deficiency of either FXII or FXI resulted in a significant and equivalent reduction in thrombus weight and incidence of thrombus formation in the IVC stenosis model. Thrombi formed in the IVC stenosis model contained significantly higher levels of citrullinated histone H3 compared to the thrombi formed in the IVC stasis model. Deletion of either FXII or FXI also resulted in a significant and equivalent reduction in both fibrin and platelet accumulation in the femoral vein electrolytic injury model.

Conclusions—Collectively, these data indicate that FXII and FXI contribute to the size of venous thrombosis in models with blood flow and thrombus composition in a stasis model. This study also demonstrates the importance of using multiple mouse models to assess the role of a given protein in venous thrombosis.

Keywords

animal models; blood coagulation; factor XI; factor XII; venous thrombosis

Corresponding Author: Nigel Mackman, Ph.D., Department of Medicine, 116 Manning Drive 8004B Mary Ellen Jones Building, University of North Carolina at Chapel Hill Chapel Hill, NC 27599, USA, nmackman@med.unc.edu, Tel: (919) 843-3961, Fax: (919) 966-6012.

Authorship Details

S.P.G and N.M designed experiments, interpreted data and wrote the manuscript. S.P.G, T.M.O and B.C.C conducted experiments, analyzed data and edited the manuscript.

Conflicts of Interest

The authors have no relevant conflicts of interest to disclose.

Introduction

Venous thromboembolism (VTE), that includes deep vein thrombosis (DVT) and pulmonary embolism (PE), is a leading cause of morbidity and mortality in the developed world [1]. Anticoagulants serve as a mainstay therapy for the prevention and treatment of VTE [2]. However, a major limitation of current anticoagulant agents is their potential to cause life-threatening bleeding [2,3]. Considerable efforts have been made to identify novel targets for anticoagulant therapies that can effectively prevent VTE while sparing critical physiological hemostatic processes [2].

The intrinsic coagulation pathway includes factors (F) XII and FXI. FXII undergoes autoactivation upon exposure to negatively-charged surfaces, such as phospholipids on damaged cells, polyphosphate, kaolin, and implantable medical device materials [4,5]. FXIIa catalyzes the activation of FXI that, in turn, activates FIX. FIXa plays a critical role in the generation of FXa and subsequently thrombin. Amplification of thrombin generation by the intrinsic pathway is important because initiation from the tissue factor (TF)-FVIIa complex is rapidly inhibited by tissue factor pathway inhibitor [6].

People with a genetic deficiency of FXII do not have a bleeding diathesis [7]. In contrast, FXI deficiency in humans is associated with a relatively mild bleeding diathesis that is most apparent on provocation in tissues with high fibrinolytic activity [8]. This contrasts with humans with deficiencies in FVIII (hemophilia A) or FIX (hemophilia B) that have a more severe phenotype with spontaneous episodes of bleeding [9]. Based, in part, on these clinical phenotypes a number of agents have been developed that target FXII and FXI [4,10–13]. It is anticipated that agents targeting these factors will cause less bleeding than conventional anticoagulants. Encouragingly, results of two recent clinical trials have demonstrated that either reducing levels of FXI or inhibiting FXIa is effective in reducing the rate of asymptomatic venous thrombosis in patients undergoing total knee arthroplasty [14,15].

Both FXII and FXI have been shown to contribute to different forms of arterial thrombosis, including myocardial ischemia and stroke in preclinical models [12,16,17]. However, there are conflicting data regarding the relative contribution of FXII and FXI to venous thrombus formation in mice. Antisense oligonucleotide mediated knockdown of either FXII or FXI was associated with reduced venous thrombosis in the St Thomas' model, which involves stenosis of the infrarenal section of the inferior vena cava (IVC) and temporary application of a neurovascular clip [18]. In contrast, a study reported that FXII deficiency, but not FXI deficiency, resulted in a significant reduction in thrombus formation in the IVC stenosis model of thrombosis without additional injury [19]. A recent consensus paper highlighted the potential for differences among models of venous thrombosis and the value of using multiple models with independent modes of initiation to assess the role of a given protein in venous thrombosis [20,21].

The goal of this study was to evaluate the contributions of FXII and FXI to venous thrombosis using genetically deficient mice in three commonly used models: IVC stenosis, IVC stasis and femoral vein electrolytic injury.

Methods

Mice

All procedures were approved by the UNC at Chapel Hill Institutional Animal Care and Use Committee and complied with National Institutes of Health guidelines. FXII and FXI deficient mice (*F12*$^{-/-}$ and *F11*$^{-/-}$) on a C57BL/6J background were obtained from Dr David Gailani (Vanderbilt University) [22,23]. Mouse genotypes were determined by polymerase chain reaction at wean and confirmed at the experimental endpoint. Surgeries were conducted on 8–12 week old male *F12*$^{-/-}$, *F11*$^{-/-}$ or appropriate littermate control mice in an operator-blinded manner.

IVC stasis model

The IVC stasis model was conducted as previously described [24,25]. Mice were anaesthetized by intraperitoneal injection of ketamine (100 mg/kg) and xylazine (10 mg/kg). A midline laparotomy was made, the bowel externalized and wrapped in wetted gauze. The IVC and adjacent aorta was mobilized by blunt dissection. Side branches were ligated using 5–0 prolene suture. Back branches were cauterized by diathermy. The IVC was then permanently ligated using 5–0 prolene suture material. Intraoperative buprenorphine was administered at a dose of 0.05 mg/kg. The peritoneum and skin were closed using 4–0 non-absorbable monofilament suture material. At 48 hours post-thrombus induction, the thrombus was removed and weighed using a microbalance.

IVC stenosis model

Mice were anaesthetized by inhalation of isoflurane gas (1.5–3%, 1 L/min O_2) for the duration of the procedure. Body temperature was maintained using a heated pad. Appropriate aseptic surgical technique was used. A midline laparotomy was made, the bowel externalized and wrapped in wetted gauze. The IVC and adjacent aorta was mobilized by blunt dissection. Side branches were first ligated using 4–0 silk suture. The IVC and aorta were separated by sharp dissection just distal to the confluence of the left renal vein and a piece of 4–0 silk suture material slung around the IVC. A piece of 5–0 prolene suture (0.1 mm diameter) was placed on the ventral surface of the IVC and the 4–0 silk suture was ligated tightly around the IVC with inclusion of the 5–0 prolene suture. The 5–0 prolene suture was removed resulting in stenosis of the IVC. Intraoperative buprenorphine was administered at a dose of 0.05 mg/kg. The peritoneum and skin were closed using 4–0 non-absorbable monofilament suture material in two layers. At 48 hours post-thrombus induction, the IVC was inspected for the presence of thrombus with any resultant thrombus removed from the IVC and weighed using a microbalance.

Femoral vein electrolytic injury model

The femoral vein electrolytic injury model was conducted as previously described [26,27]. Mice were anaesthetized by intraperitoneal injection of pentobarbital (50 mg/kg). Rhodamine 6G (0.5 μg/g) and Alexa-647 labelled anti-fibrin antibody (clone 59D8, 1 μg/g) were administered intravenously through the external jugular vein. The femoral vein was exposed by a groin incision. A 1.5V charge was applied to the ventral surface of the femoral

vein for 30 seconds using a grounded 75 μm microsurgical needle. Accumulation of platelets and fibrin was imaged by fluorescence intravital videomicroscopy in which the field was illuminated by beam expanded 532-nm and 650-nm laser light and fluorescent signal visualized using an operating microscope (M-690, Wild/Leica, Germany) equipped with a digital camera (DVC-1412, DVC Inc, TX) connected to a camera-synchronized shutter (UniBlitz, Chroma Technology, VT). Data were analyzed using ImageJ software (v1.52, National Institute of Health, MD) and normalized fluorescent intensities calculated.

Western blotting

Western blotting of thrombus lysates was conducted as previously described [25]. Thrombi from wildtype mice on a C57BL/6J background were harvested, snap frozen and stored at −80°C prior to processing. Thrombi were homogenized in radioimmunoprecipitation buffer (EMD Millipore, Germany) supplemented with a protease inhibitor cocktail (Complete, Roche, Switzerland) and incubated on ice for 30 minutes. Lysates were clarified by centrifugation at 15,000×g for 15 minutes at 4°C. Total soluble protein concentration was determined using a bicinchoninic acid assay (Pierce, MA). Lysates were prepared for electrophoresis by addition of SDS sample buffer (Invitrogen, CA) and heated to 95°C for 10 minutes. Equal amounts of total soluble protein from thrombus lysates were loaded onto 4–20% gradient SDS polyacrylamide gels (BioRad, CA) and separated by electrophoresis. Proteins were transferred to polyvinylidene difluoride membranes and blocked using protein-free blocking buffer (Thermo Fisher Scientific, MA). Membranes were probed with anti-CD41 (PA5–79527, Thermo Fisher Scientific, MA, 0.5 μg/ml), anti-Ly6G (1A8, Lifespan Biosciences, WA, 2 μg/ml), anti-H3Cit (ab5103, Abcam, MA, 1μg/ml), anti-H3 (ab1791, Abcam, MA, 0.5 μg/ml), anti-β actin (SC-47778, Santa Cruz, CA, 1 μg/ml) or anti-fibrin(ogen) (A0080, Dako, Japan, 1μg/ml) primary antibodies. Membranes were probed with Alexa-700 and Alexa-800 conjugated anti-IgG secondary antibodies (Invitrogen, CA, 0.1 μg/ml) and antigen-antibody complexes visualized on an Odyssey imaging system (Li-Cor Biosciences, NE). Densitometric analysis was conducted using ImageJ software (version 1.52, National Institute of Health, MD).

Statistical Analysis

Shapiro-Wilk normality tests were used to assess normality of data with parametric and nonparametric tests selected as appropriate. For analysis of two groups either unpaired Student’s t-tests or Mann-Whitney U tests were used. To assess differences in the incidence of thrombus formation between groups the Fisher Exact test was used. Data were analyzed using Prism software (v8.2, Graphpad, CA).

Results

Effect of FXII or FXI deficiency on venous thrombosis in the IVC stasis and stenosis models

To determine the contribution of FXII and FXI to venous thrombosis, we subjected gene-specific knockout mice to the IVC stasis and the IVC stenosis models. It is important to note the *F12*$^{-/-}$ and *F11*$^{-/-}$ mice have normal levels of white blood cells and platelets [28,29]. In the IVC stasis model, FXII deficiency did not affect thrombus weight at 48 hrs post-induction

(Figure 1A). Similarly, *F11*$^{-/-}$ mice subject to the IVC stasis model demonstrated a small (12%) but non-significant reduction in thrombus weight at 48 hrs post-induction compared to *F11*$^{+/+}$ controls (Figure 1B).

In the IVC stenosis model, in which the thrombus forms in the presence of blood flow, a significant reduction in thrombus weight at 48 hrs post-induction was observed in *F12*$^{-/-}$ mice compared to *F12*$^{+/+}$ littermate controls (Figure 1C). The incidence of thrombus formation was also significantly lower in *F12*$^{-/-}$ mice compared to *F12*$^{+/+}$ controls (3/11 vs 10/12) (Figure 1D). Thrombus weight at 48 hrs post-induction was also significantly reduced in *F11*$^{-/-}$ mice compared to *F11*$^{+/+}$ littermate controls subject to the IVC stenosis model (Figure 1E). Consistent with impaired thrombus formation in *F11*$^{-/-}$ mice, the incidence of thrombus was significantly reduced compared to *F11*$^{+/+}$ littermate controls (4/12 vs 11/14) (Figure 1F).

Assessment of thrombus composition in the IVC stasis and stenosis models

We determined if differences in thrombus composition could explain why FXII and FXI contributed to the IVC stenosis model but not the IVC stasis model. The composition of thrombi formed in wild-type mice using the two models was assessed by western blotting (Figure 2A). Thrombi formed in the IVC stenosis and stasis models contained similar levels of fibrin(ogen) (Figure 2B). To determine the relative abundance of platelets and neutrophils thrombus tissue lysates were immunoblotted for the cell specific markers CD41 and Ly6G, respectively. Surprisingly, densitometric analysis revealed that the platelet marker CD41 and the neutrophil marker Ly6G were more abundant in thrombi formed in the IVC stasis model compared to thrombi formed in the IVC stenosis model (Figure 2C and D). The relative abundance of β actin was not found to differ significantly between thrombi formed in the two models indicating a similar degree of cellularity (Figure 2E). To assess NET formation in thrombi the abundance of citrullinated histone H3 was assessed together with histone H3 as a control. Interestingly, both citrullinated histone H3 and histone H3 were more abundant in thrombi formed by the IVC stenosis compared to the IVC stasis model (Figure 2F and G). The ratio of citrullinated histone H3 to histone H3 was also significantly increased in thrombi formed in the IVC stenosis model compared to the IVC stasis model (Figure 2H).

The composition of thrombi formed in *F12*$^{-/-}$ and *F11*$^{-/-}$ mice using the IVC stenosis and IVC stasis model was also assessed by western blotting. Consistent with findings in wild-type mice, there was no difference in the relative abundance of fibrin(ogen) and β actin, and the relative abundance of citrullinated histone H3, total histone H3 and the ratio of citrullinated histone H3 to total histone H3 were all markedly elevated in thrombi formed using the IVC stenosis model (Figure S1). In contrast to the results with wild-type mice, there was no significant difference in the relative abundance of CD41 or Ly6G (Figure S1).

To determine if loss of FXII or FXI altered the composition of thrombi formed using the IVC stasis model, composition of thrombi formed in *F12*$^{-/-}$ and *F11*$^{-/-}$ mice was compared to the respective wild-type littermate controls. Interestingly, there was a significant decrease in levels of fibrin(ogen) in thrombi formed in *F12*$^{-/-}$ mice and *F11*$^{-/-}$ mice compared with their respective controls (Figure 3A and H). No significant difference in the relative abundance of CD41, Ly6G or β actin was observed in thrombi formed in *F12*$^{-/-}$ mice

compared to *F12*$^{+/+}$ mice (Figure 3B–D) and *F11*$^{-/-}$ mice compared to *F11*$^{+/+}$ mice (Figure 3I–K). A significant increase in both citrullinated histone H3 and total histone H3 was observed in thrombi formed in *F11*$^{-/-}$ mice compared to *F11*$^{+/+}$ controls (Figure 3L and M). Similarly, a trend towards increased levels of citrullinated histone H3 and total histone H3 was observed in thrombi formed in *F12*$^{-/-}$ mice compared to *F12*$^{+/+}$ controls (Figure 3E and F). Interestingly, a trend towards a reduced ratio of citrullinated histone H3 to total histone H3 was observed in thrombi formed in *F12*$^{-/-}$ mice (Figure 3G), but not *F11*$^{-/-}$ mice (Figure 3N), when compared to the respective controls.

Effect of FXII and FXI deficiency on thrombus formation in the electrolytic injury model

To assess the contribution of FXII and FXI in an additional model of venous thrombosis with preserved blood flow, *F12*$^{-/-}$, *F11*$^{-/-}$ and appropriate wild-type littermate control mice were subjected to the femoral vein electrolytic injury model. A marked reduction in the accumulation of fibrin was observed in *F12*$^{-/-}$ mice compared to *F12*$^{+/+}$ littermate controls (Figure 4A). Quantification of the data by calculation of fibrin area under the curve (AUC) demonstrated a significant 85% reduction in the accumulation of fibrin (Figure 4B). A significant reduction in the accumulation of platelets was also observed in *F12*$^{-/-}$ mice compared to *F12*$^{+/+}$ littermate controls (Figure 4C and 4D). In *F11*$^{-/-}$ mice, a marked reduction in fibrin accumulation was observed in *F11*$^{-/-}$ mice compared to *F11*$^{+/+}$ littermates (Figure 4E). Quantification revealed a significant 88% reduction in fibrin accumulation was observed in *F11*$^{-/-}$ mice compared to *F11*$^{+/+}$ littermates (Figure 4F). Furthermore, accumulation of platelets was also significantly reduced (Figure 4G and 4H).

Discussion

In this study, we found a model-dependent contribution of FXII and FXI to venous thrombosis in mice. In the IVC stasis model neither FXII nor FXI deficiency conferred protection from venous thrombus formation. The IVC stasis model provides a strong thrombogenic insult owing to the complete ligation of the IVC, the ligation of distal lateral IVC side branches, and the cauterization of back branches. The cauterization of back branches and the full ligation of the IVC in this model likely exposes significant amounts of subendothelial TF that may trigger thrombosis [30]. Indeed, vessel wall TF, but not myeloid cell TF, has been shown to drive thrombosis in the IVC stasis model, whereas myeloid cell TF contributes to thrombosis in the IVC stenosis model [19,30,31]. It is, therefore, not surprising that a role for FXII and FXI cannot be detected in this model. Moreover, it has previously been shown that the IVC stasis model is insensitive to neutrophil depletion, platelet depletion or inhibition of platelet activation [32,33]. Interestingly, however, we found that an absence of either FXII or FXI was associated with decreased levels of fibrin(ogen) and increased levels of citrullinated histone H3.

In the IVC stenosis model deletion of either FXII or FXI resulted in a comparable reduction in venous thrombus formation. The result with FXI deficient mice contrasts to a previous report that found no role for FXI in venous thrombus formation using genetically-deficient mice subject to the IVC stenosis model (Table 1) [19]. However, the absence of a phenotype in *F11*$^{-/-}$ mice in the von Brühl *et. al.* study may be due to a number of factors that include use

of a small number of *F11*$^{-/-}$ mice in an inherently variable model and a control group that were not littermates[34]. In contrast to the IVC stasis model, myeloid TF, neutrophils, NETs and platelets have all been found to contribute to thrombus formation with IVC stenosis, a model in which the thrombus forms in the presence of blood flow and provides a milder thrombogenic insult [19,32,33,35,36].

We determined if compositional changes in the thrombus may have contributed to the sensitivity of the IVC stenosis model to FXII and FXI. Given the important role of even relatively low shear rates for platelet activation, we hypothesized that the IVC stenosis model, which maintains low levels of blood flow at the time of induction, would support more platelet activation and incorporation than the IVC stasis model. Platelets can release and bind polyphosphate that supports activation of FXII [37]. In addition, the activated platelet surface has also been shown to promote generation of FXIIa through exposure of phosphatidylserine and to be an important surface for the activation of FXI [38–41]. Surprisingly, immunoblotting revealed a significantly lower relative abundance of the platelet surface marker CD41 in thrombi formed using the IVC stenosis model compared to the IVC stasis model suggesting a relatively lower abundance of platelets. Based on this finding it is unlikely that differences in platelet accumulation accounted for the observed sensitivity of the IVC stenosis model to FXII and FXI.

Surprisingly, the relative abundance of the neutrophil marker Ly6G was significantly lower in thrombi formed in the IVC stenosis model when compared to the IVC stasis model indicating a lower neutrophil content. Based on the potential involvement of NET formation in FXIIa-dependent thrombus propagation, we evaluated the extent of NET formation in the two models by measuring levels of the NET marker citrullinated histone H3 as a function of total histone H3 [25]. Protein arginine deiminase 4 PAD4 citrullinates histone H3 and drives NETosis, a process that has been found to be required for venous thrombosis in the IVC stenosis model [35]. We observed significantly higher levels of both total histone H3 and citrullinated histone H3 in thrombi formed in the IVC stenosis model than the IVC stasis model. The higher histone H3 content of thrombi from the IVC stenosis model is consistent with increased nucleated cell content. Critically, the ratio of citrullinated histone H3 to total histone H3 was significantly higher in thrombi formed using the IVC stenosis model compared to the IVC stasis model. This suggests that the amount of NET formation is higher in the IVC stenosis model. The contribution of NETs to activation of FXII remains unclear. Purified DNA has been found to promote formation of FXIIa and FXIa [42–44]. Isolated histones can also promote FXIIa generation in a direct or indirect manner [44,45]. However, there are mixed reports on the ability of intact NETs to activate FXII [44,46]. It is interesting to consider if NET mediated activation of FXII could have contributed to the observed sensitivity of the IVC stenosis model to these factors.

The composition of thrombi formed in FXII and FXI deficient mice using either the IVC stenosis or IVC stasis models was also assessed by western blotting. In contrast to our findings in thrombi formed in wild-type mice we did not observe differences in the relative abundance of CD41 or Ly6G. It is possible that deficiencies in FXII and FXI alter the recruitment of platelets and neutrophils that could account for this discordant observation. Importantly, however, as observed in wild-type thrombi a markedly higher relative

abundance of citrullinated H3, total histone H3 and an increased citrullinated H3 to total H3 ratio was observed FXII and FXI deficient thrombi formed using the stenosis model versus the stasis model. This complementary finding further reinforces the potential importance of NET formation to venous thrombus formation in the IVC stenosis model.

In addition to the ability of NETs to function as a surface for the activation of FXII, it has recently been demonstrated that FXII serves as an activator of neutrophils promoting the formation of NETs [47]. Furthermore, neutrophils express FXII that represents a distinct pool of FXII that cannot be compensated for by plasma FXII derived from hepatic expression [47]. To investigate the potential of FXII to modulate thrombus NET formation the composition of thrombi formed using the IVC stasis model was assessed in $F12^{-/-}$ mice and compared to respective $F12^{+/+}$ controls. Thrombi formed in $F11^{-/-}$ and $F11^{+/+}$ mice were used to control for a non-FXII selective contribution of the intrinsic pathway. Consistent with a role for FXII as an enhancer of NET formation, thrombi formed in $F12^{-/-}$ mice, but not $F11^{-/-}$ mice, demonstrated a reduced ratio of citrullinated H3 to total H3. Further work is required to determine if the observed effect of FXII on NET formation contributes to the observed protection of FXII deficient mice in intrinsic pathway sensitive models of venous thrombosis.

A deficiency of either FXII or FXI did not affect thrombus weight in the IVC stasis model. However, we observed a significant decrease in fibrin(ogen) and a significant increase in citrullinated H3 in thrombi formed in $F11^{-/-}$ mice compared with controls using the IVC stasis model. Similar results were observed with $F12^{-/-}$ mice. It is possible that an increase in NET formation may compensate for the reduction in fibrin(ogen). Fibrin(ogen) binds to the integrin αMβ2 on the surface of leukocytes [48]. In addition, platelet binding to neutrophils via an interaction between GP1bα and αMβ2 enhances NET formation [49–51]. In wild-type mice, fibrin(ogen) binding to αMβ2 on neutrophils may limit NET formation whereas in $F12^{-/-}$ mice *and* $F11^{-/-}$ mice more αMβ2 is available to bind platelet with a subsequent increase in NET formation.

Thrombus formation in the IVC stenosis model takes place in the presence of residual blood flow. Experimental measurements have demonstrated that at the time of initiation blood flow through the IVC is reduced by 80–90% in the stenosis model compared to a complete absence of blood flow observed in the stasis model [19,52,53]. However, histological analysis indicates that in wild-type mice an occlusive thrombus forms by 24 hrs [19]. It is possible in FXII or FXI deficient mice that a failure to form an initial occlusive thrombus also have continued blood flow through the vessel. The retention of blood flow in the stenosed vessel may prevent the prolonged residency of procoagulant proteins and cells and subsequent amplification of thrombus formation.

To further evaluate the contribution of FXII and FXI to venous thrombosis in a flow competent model, gene-specific knockout mice were assessed using the femoral vein electrolytic injury model of thrombosis. The femoral vein electrolytic injury model has an independent mode of initiation compared to the IVC stenosis and IVC stasis model with iron based electrolytic vascular injury driving formation of a fibrin and platelet rich thrombus [26]. Both coagulation proteases and platelets contribute to thrombus formation in this model

[26,27,54]. The femoral vein electrolytic injury model has previously been shown to be sensitive to deletion of intrinsic pathway FIX [26,55]. Further, inhibition of polyphosphate, a potential physiological activator of FXII, markedly reduced thrombus formation in the femoral vein electrolytic injury model [56]. Importantly, deletion of either FXII or FXI impaired thrombus formation to a similar extent in this model. This is consistent with data in the IVC stenosis model and suggests that both FXII and FXI are important drivers of venous thrombosis. It is interesting to consider if the presence of residual and preserved blood flow in the IVC stenosis and femoral vein electrolytic injury models may have contributed to the observed sensitivity to FXII and FXI. In microfluidic chamber-based studies the formation of NETs has been found to occur in a shear stress dependent manner [57]. Shear stress in the IVC stenosis model and femoral vein electrolytic injury model may be an important driver of NET formation. The presence of NET components at the site of thrombosis in these models could provide a surface for activation of FXII.

There has been considerable discussion about the benefits of targeting FXII versus FXI for preventing venous thrombosis in patients [10]. In the baboon femoral arterio-venous shunt model inhibition of FXI-dependent activation of FIX reduced platelet deposition within the collagen-coated portion of shunt whereas inhibition of either FXII activation of FXI or FXII failed to reduce platelet deposition [58–60]. The IVC stenosis and stasis models of venous thrombosis are not titratable making it challenging to assess the relative contribution of components of the intrinsic pathways. A single dose of antisense oligonucleotide mediated knockdown of either FXII or FXI produced similar reductions in both the St Thomas' model and the ferric chloride IVC model [18]. Importantly, siRNA mediated FXII knockdown to intermediate levels, but not high levels, was more protective than equivalent levels of FXI knockdown in the femoral vein electrolytic injury model (Table 1)[61]. These findings suggest that there may be differential requirements for FXII and FXI during venous thrombosis in mice.

Our study indicates that FXII and FXI have similar contributions to three mouse models of venous thrombosis. In humans FXI appears to play a greater role than FXII in various forms of thrombosis, including VTE [10]. In contrast to these clinical observations FXII deficient mice have consistently been found to be protected in models of both venous and arterial thrombosis [16]. These discordant findings suggest a limitation of mouse models for studying the role of FXII in thrombosis because they may be overly dependent on contact activation mediated thrombus formation. To conclude, the results of this study have revealed model-dependent contributions of FXII and FXI to venous thrombus formation in mice.

Supplementary Material

Refer to Web version on PubMed Central for supplementary material.

Acknowledgements

The authors thank Ying Zhang for excellent technical assistance and helpful comments from Dr. Silvio Antoniak (University of North Carolina at Chapel Hill) and Dr. David Gailani (Vanderbilt University). This work was supported by an AHA postdoctoral fellowship 19POST34370026 (S.P.G), the NIH NHLBI R01HL147149 (N.M) and the John C. Parker professorship (N.M).

References

1. Wendelboe AM, McCumber M, Hylek EM, et al. Global public awareness of venous thromboembolism. J Thromb Haemost. 2015;13(8):1365–1371. [PubMed: 26084415]
2. Mackman N, Bergmeier W, Stouffer GA, Weitz JI. Therapeutic strategies for thrombosis: new targets and approaches. Nat Rev Drug Discov. 2020.
3. Weitz JI, Chan NC. Advances in Antithrombotic Therapy. Arterioscler Thromb Vasc Biol. 2019;39(1):7–12. [PubMed: 30580558]
4. Grover SP, Mackman N. Intrinsic Pathway of Coagulation and Thrombosis. Arterioscler Thromb Vasc Biol. 2019:ATVBAHA118312130.
5. Gailani D, Geng Y, Verhamme I, et al. The mechanism underlying activation of factor IX by factor XIa. Thromb Res. 2014;133 Suppl 1:S48–51. [PubMed: 24759143]
6. Grover SP, Mackman N. Tissue Factor: An Essential Mediator of Hemostasis and Trigger of Thrombosis. Arterioscler Thromb Vasc Biol. 2018;38(4):709–725. [PubMed: 29437578]
7. Lämmle B, Wuillemin WA, Huber I, et al. Thromboembolism and bleeding tendency in congenital factor XII deficiency--a study on 74 subjects from 14 Swiss families. Thromb Haemost. 1991;65(2):117–121. [PubMed: 1905067]
8. Bolton-Maggs PH. Factor XI deficiency and its management. Haemophilia. 2000;6 Suppl 1:100–109. [PubMed: 10982275]
9. Bolton-Maggs PH, Pasi KJ. Haemophilias A and B. Lancet. 2003;361(9371):1801–1809. [PubMed: 12781551]
10. Gailani D, Bane CE, Gruber A. Factor XI and contact activation as targets for antithrombotic therapy. J Thromb Haemost. 2015;13(8):1383–1395. [PubMed: 25976012]
11. Weitz JI, Fredenburgh JC. Factors XI and XII as Targets for New Anticoagulants. Front Med (Lausanne). 2017;4:19. [PubMed: 28286749]
12. Nickel KF, Long AT, Fuchs TA, Butler LM, Renné T. Factor XII as a Therapeutic Target in Thromboembolic and Inflammatory Diseases. Arterioscler Thromb Vasc Biol. 2017;37(1):13–20. [PubMed: 27834692]
13. Mackman N, Bergmeier W, Stouffer GA, Weitz JI. Therapeutic strategies for thrombosis: new targets and approaches. Nat Rev Drug Discov. 2020;19(5):333–352. [PubMed: 32132678]
14. Büller HR, Bethune C, Bhanot S, et al. Factor XI antisense oligonucleotide for prevention of venous thrombosis. N Engl J Med. 2015;372(3):232–240. [PubMed: 25482425]
15. Weitz JI, Bauersachs R, Becker B, et al. Effect of Osocimab in Preventing Venous Thromboembolism Among Patients Undergoing Knee Arthroplasty: The FOXTROT Randomized Clinical Trial. JAMA. 2020;323(2):130–139. [PubMed: 31935028]
16. Grover SP, Mackman N. Intrinsic Pathway of Coagulation and Thrombosis. Arterioscler Thromb Vasc Biol. 2019;39(3):331–338. [PubMed: 30700128]
17. Gailani D, Gruber A. Factor XI as a Therapeutic Target. Arterioscler Thromb Vasc Biol. 2016;36(7):1316–1322. [PubMed: 27174099]
18. Revenko AS, Gao D, Crosby JR, et al. Selective depletion of plasma prekallikrein or coagulation factor XII inhibits thrombosis in mice without increased risk of bleeding. Blood. 2011;118(19):5302–5311. [PubMed: 21821705]
19. von Brühl ML, Stark K, Steinhart A, et al. Monocytes, neutrophils, and platelets cooperate to initiate and propagate venous thrombosis in mice in vivo. J Exp Med. 2012;209(4):819–835. [PubMed: 22451716]
20. Diaz JA, Saha P, Cooley B, et al. Choosing a Mouse Model of Venous Thrombosis. Arterioscler Thromb Vasc Biol. 2019:ATVBAHA118311818.
21. Diaz JA, Saha P, Cooley B, et al. Choosing a mouse model of venous thrombosis: a consensus assessment of utility and application. J Thromb Haemost. 2019;17(4):699–707. [PubMed: 30927321]
22. Pauer HU, Renné T, Hemmerlein B, et al. Targeted deletion of murine coagulation factor XII gene-a model for contact phase activation in vivo. Thromb Haemost. 2004;92(3):503–508. [PubMed: 15351846]

23. Gailani D, Lasky NM, Broze GJ. A murine model of factor XI deficiency. Blood Coagul Fibrinolysis. 1997;8(2):134–144. [PubMed: 9518045]
24. Hisada Y, Ay C, Auriemma AC, Cooley BC, Mackman N. Human pancreatic tumors grown in mice release tissue factor-positive microvesicles that increase venous clot size. J Thromb Haemost. 2017;15(11):2208–2217. [PubMed: 28834179]
25. Hisada Y, Grover SP, Maqsood A, et al. Neutrophils and neutrophil extracellular traps enhance venous thrombosis in mice bearing human pancreatic tumors. Haematologica. 2020;105(1):218–225. [PubMed: 31048354]
26. Cooley BC. In vivo fluorescence imaging of large-vessel thrombosis in mice. Arterioscler Thromb Vasc Biol. 2011;31(6):1351–1356. [PubMed: 21393581]
27. Aleman MM, Walton BL, Byrnes JR, et al. Elevated prothrombin promotes venous, but not arterial, thrombosis in mice. Arterioscler Thromb Vasc Biol. 2013;33(8):1829–1836. [PubMed: 23723374]
28. Tucker EI, Gailani D, Hurst S, Cheng Q, Hanson SR, Gruber A. Survival advantage of coagulation factor XI-deficient mice during peritoneal sepsis. J Infect Dis. 2008;198(2):271–274. [PubMed: 18491973]
29. Renné T, Pozgajová M, Grüner S, et al. Defective thrombus formation in mice lacking coagulation factor XII. J Exp Med. 2005;202(2):271–281. [PubMed: 16009717]
30. Day SM, Reeve JL, Pedersen B, et al. Macrovascular thrombosis is driven by tissue factor derived primarily from the blood vessel wall. Blood. 2005;105(1):192–198. [PubMed: 15339841]
31. Hampton AL, Diaz JA, Hawley AE, et al. Myeloid cell tissue factor does not contribute to venous thrombogenesis in an electrolytic injury model. Thromb Res. 2012;130(4):640–645. [PubMed: 22192154]
32. El-Sayed OM, Dewyer NA, Luke CE, et al. Intact Toll-like receptor 9 signaling in neutrophils modulates normal thrombogenesis in mice. J Vasc Surg. 2016;64(5):1450–1458.e1451. [PubMed: 26482993]
33. Payne H, Ponomaryov T, Watson SP, Brill A. Mice with a deficiency in CLEC-2 are protected against deep vein thrombosis. Blood. 2017;129(14):2013–2020. [PubMed: 28104688]
34. Geddings J, Aleman MM, Wolberg A, von Brühl ML, Massberg S, Mackman N. Strengths and weaknesses of a new mouse model of thrombosis induced by inferior vena cava stenosis: communication from the SSC of the ISTH. J Thromb Haemost. 2014;12(4):571–573. [PubMed: 24460606]
35. Martinod K, Demers M, Fuchs TA, et al. Neutrophil histone modification by peptidylarginine deiminase 4 is critical for deep vein thrombosis in mice. Proc Natl Acad Sci U S A. 2013;110(21):8674–8679. [PubMed: 23650392]
36. Brill A, Fuchs TA, Savchenko AS, et al. Neutrophil extracellular traps promote deep vein thrombosis in mice. J Thromb Haemost. 2012;10(1):136–144. [PubMed: 22044575]
37. Verhoef JJ, Barendrecht AD, Nickel KF, et al. Polyphosphate nanoparticles on the platelet surface trigger contact system activation. Blood. 2017;129(12):1707–1717. [PubMed: 28049643]
38. Bäck J, Sanchez J, Elgue G, Ekdahl KN, Nilsson B. Activated human platelets induce factor XIIa-mediated contact activation. Biochem Biophys Res Commun. 2010;391(1):11–17. [PubMed: 19878657]
39. Van Der Meijden PE, Van Schilfgaarde M, Van Oerle R, Renné T, ten Cate H, Spronk HM. Platelet- and erythrocyte-derived microparticles trigger thrombin generation via factor XIIa. J Thromb Haemost. 2012;10(7):1355–1362. [PubMed: 22537188]
40. Zakharova NV, Artemenko EO, Podoplelova NA, et al. Platelet surface-associated activation and secretion-mediated inhibition of coagulation factor XII. PLoS One. 2015;10(2):e0116665. [PubMed: 25688860]
41. Chaudhry SA, Serrata M, Tomczak L, et al. Cationic Zinc is Required for Factor XII Recruitment and Activation by Stimulated Platelets and for Thrombus Formation in vivo. J Thromb Haemost. 2020.
42. Kannemeier C, Shibamiya A, Nakazawa F, et al. Extracellular RNA constitutes a natural procoagulant cofactor in blood coagulation. Proc Natl Acad Sci U S A. 2007;104(15):6388–6393. [PubMed: 17405864]

43. Vu TT, Leslie BA, Stafford AR, Zhou J, Fredenburgh JC, Weitz JI. Histidine-rich glycoprotein binds DNA and RNA and attenuates their capacity to activate the intrinsic coagulation pathway. Thromb Haemost. 2016;115(1):89–98. [PubMed: 26354857]
44. Noubouossie DF, Whelihan MF, Yu YB, et al. In vitro activation of coagulation by human neutrophil DNA and histone proteins but not neutrophil extracellular traps. Blood. 2017;129(8):1021–1029. [PubMed: 27919911]
45. Semeraro F, Ammollo CT, Morrissey JH, et al. Extracellular histones promote thrombin generation through platelet-dependent mechanisms: involvement of platelet TLR2 and TLR4. Blood. 2011;118(7):1952–1961. [PubMed: 21673343]
46. Oehmcke S, Mörgelin M, Herwald H. Activation of the human contact system on neutrophil extracellular traps. J Innate Immun. 2009;1(3):225–230. [PubMed: 20375580]
47. Stavrou EX, Fang C, Bane KL, et al. Factor XII and uPAR upregulate neutrophil functions to influence wound healing. J Clin Invest. 2018;128(3):944–959. [PubMed: 29376892]
48. Flick MJ, LaJeunesse CM, Talmage KE, et al. Fibrin(ogen) exacerbates inflammatory joint disease through a mechanism linked to the integrin alphaMbeta2 binding motif. J Clin Invest. 2007;117(11):3224–3235. [PubMed: 17932565]
49. Sreeramkumar V, Adrover JM, Ballesteros I, et al. Neutrophils scan for activated platelets to initiate inflammation. Science. 2014;346(6214):1234–1238. [PubMed: 25477463]
50. Jimenez MA, Novelli E, Shaw GD, Sundd P. Glycoprotein Ibα inhibitor (CCP-224) prevents neutrophil-platelet aggregation in Sickle Cell Disease. Blood Adv. 2017;1(20):1712–1716. [PubMed: 28966995]
51. Pulavendran S, Rudd JM, Maram P, et al. Combination Therapy Targeting Platelet Activation and Virus Replication Protects Mice against Lethal Influenza Pneumonia. Am J Respir Cell Mol Biol. 2019;61(6):689–701. [PubMed: 31070937]
52. Aghourian MN, Lemarié CA, Blostein MD. In vivo monitoring of venous thrombosis in mice. J Thromb Haemost. 2012;10(3):447–452. [PubMed: 22212403]
53. Saha P, Andia ME, Modarai B, et al. Magnetic resonance T1 relaxation time of venous thrombus is determined by iron processing and predicts susceptibility to lysis. Circulation. 2013;128(7):729–736. [PubMed: 23820077]
54. Cooley BC, Szema L, Chen CY, Schwab JP, Schmeling G. A murine model of deep vein thrombosis: characterization and validation in transgenic mice. Thromb Haemost. 2005;94(3):498–503. [PubMed: 16268462]
55. Cooley B, Funkhouser W, Monroe D, et al. Prophylactic efficacy of BeneFIX vs Alprolix in hemophilia B mice. Blood. 2016;128(2):286–292. [PubMed: 27106122]
56. Smith SA, Choi SH, Collins JN, Travers RJ, Cooley BC, Morrissey JH. Inhibition of polyphosphate as a novel strategy for preventing thrombosis and inflammation. Blood. 2012;120(26):5103–5110. [PubMed: 22968458]
57. Yu X, Tan J, Diamond SL. Hemodynamic force triggers rapid NETosis within sterile thrombotic occlusions. J Thromb Haemost. 2018;16(2):316–329. [PubMed: 29156107]
58. Tucker EI, Marzec UM, White TC, et al. Prevention of vascular graft occlusion and thrombus-associated thrombin generation by inhibition of factor XI. Blood. 2009;113(4):936–944. [PubMed: 18945968]
59. Geng Y, Verhamme IM, Messer A, et al. A sequential mechanism for exosite-mediated factor IX activation by factor XIa. J Biol Chem. 2012;287(45):38200–38209. [PubMed: 22961984]
60. Cheng Q, Tucker EI, Pine MS, et al. A role for factor XIIa-mediated factor XI activation in thrombus formation in vivo. Blood. 2010;116(19):3981–3989. [PubMed: 20634381]
61. Liu J, Cooley B, Butler J. Reduction of hepatic Factor XII expression in mice by ALN-F12 inhibits thrombosis without increasing bleeding risk. Res Prac Thromb Haemost. 2017;1:36.

Essentials

- FXII or FXI deficient mice were subjected to three models of venous thrombosis
- FXII and FXI contributed to venous thrombus formation in models with blood flow
- A deficiency of either FXII or FXI resulted in a similar protection against venous thrombosis
- FXII and FXI deficiency altered thrombus composition in a stasis model

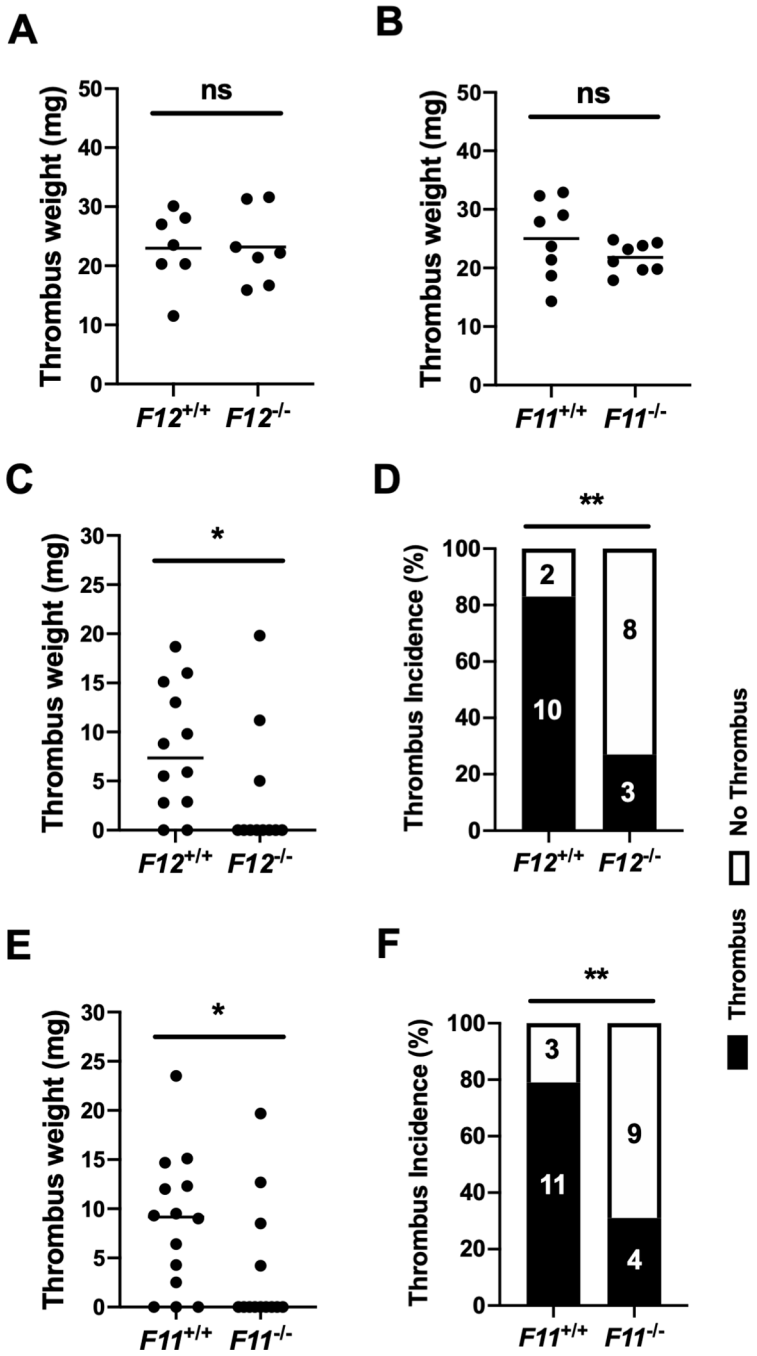

Figure 1: Effect of FXII and FXI deficiency on venous thrombus formation in the mouse IVC stasis and IVC stenosis models

FXII and FXI deficient mice were subject to the IVC stasis model or IVC stenosis models of venous thrombosis and compared to wildtype littermate controls. (A) Thrombus weight at 48 hours post-induction did not differ significantly between *F12*$^{-/-}$ mice and *F12*$^{+/+}$ controls in the IVC stasis model (n=7 per group). (B) In the IVC stasis model a small non-significant decrease in thrombus weight was observed in *F11*$^{-/-}$ mice compared to *F11*$^{+/+}$ controls (n=8 per group). ns P>0.05 Student's t-test. Thrombus weight data is represented as individual values with a line for the mean. (C) In the IVC stenosis model *F12*$^{-/-}$ mice demonstrated a

significant reduction in median thrombus weight at 48 hours post-induction compared to $F12^{+/+}$ controls (n=11–12 per group). (D) A significant reduction in the incidence of venous thrombus formation in $F12^{-/-}$ mice was observed compared to $F12^{+/+}$ controls. (E) $F11^{-/-}$ mice subject to the IVC stenosis model demonstrated a significant reduction in median thrombus weight at 48 hours post-induction compared to $F11^{+/+}$ controls (n=13–14 per group). (F) A significant reduction in the incidence of venous thrombus formation in $F11^{-/-}$ mice was observed compared to $F11^{+/+}$ controls. * P<0.05, Mann-Whitney U test, **P<0.05 Fischer's exact test. Thrombus weight data is represented as individual values with a line for the median.

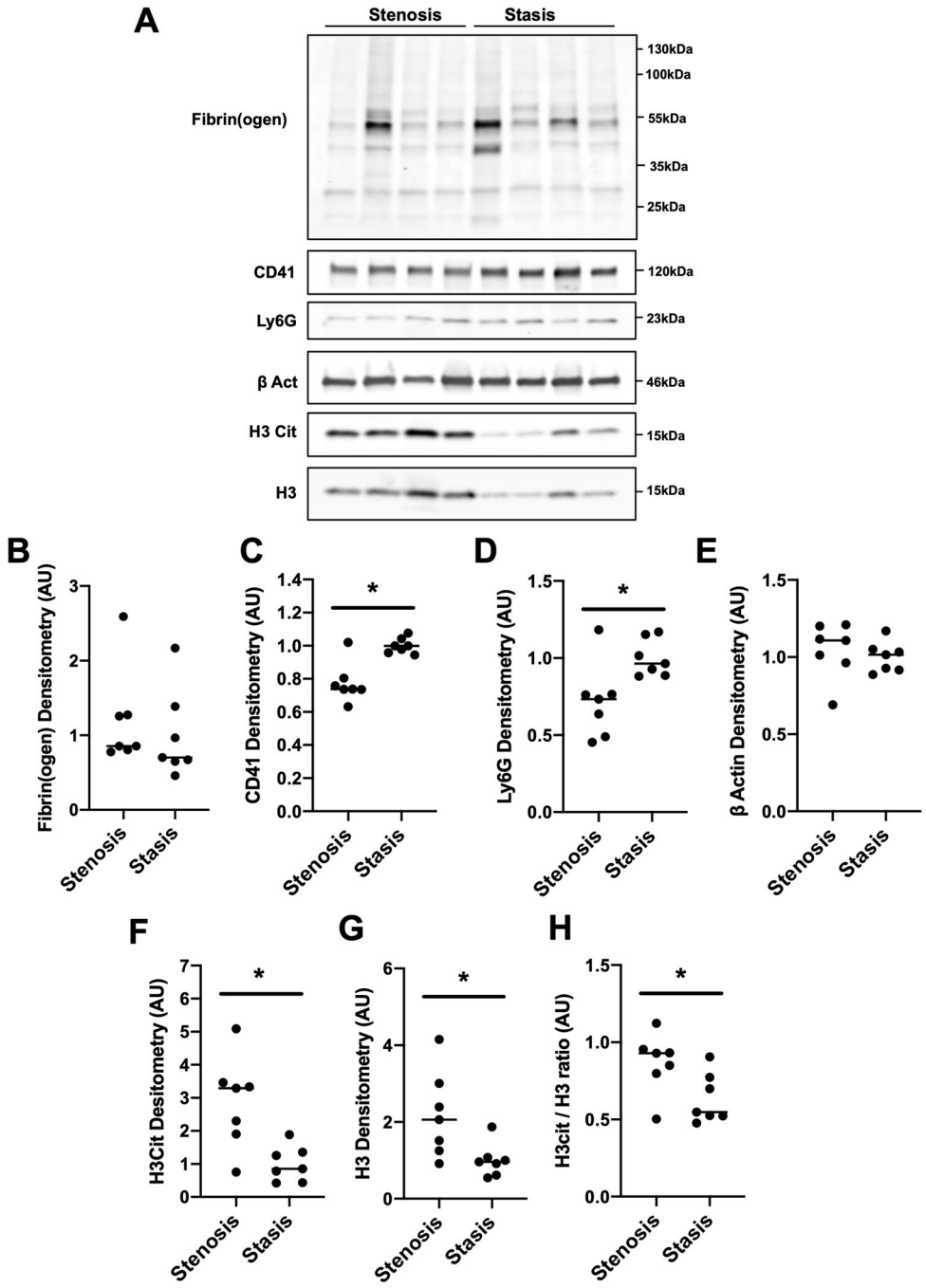

Figure 2: Composition of thrombi formed using the mouse IVC stenosis and stasis models of thrombosis

Thrombus composition was assessed by western blotting of total soluble protein lysates from thrombi formed using the IVC stenosis and IVC stasis models of thrombosis (n=7 per group). (A) Representative western blots for fibrin(ogen), the platelet marker CD41, the neutrophil marker Ly6G, the cytoplasmic marker β Actin, citrullinated histone H3 (H3Cit) and the nuclear marker total histone H3 (H3) in thrombi formed using the IVC stenosis and IVC stasis models. Densitometric analysis of (B) fibrin(ogen), (C) CD41, (D) Ly6G, (E) β Actin, (F) H3Cit and (G) H3 in thrombi formed in the IVC stenosis model compared to the

IVC stasis model. (H) The ratio of H3Cit to total H3 was significantly higher in thrombi formed in the IVC stenosis model compared to the IVC stasis model. * P<0.05, **P<0.01 Mann-Whitney U test. Data represented as individual values with a line for the median.

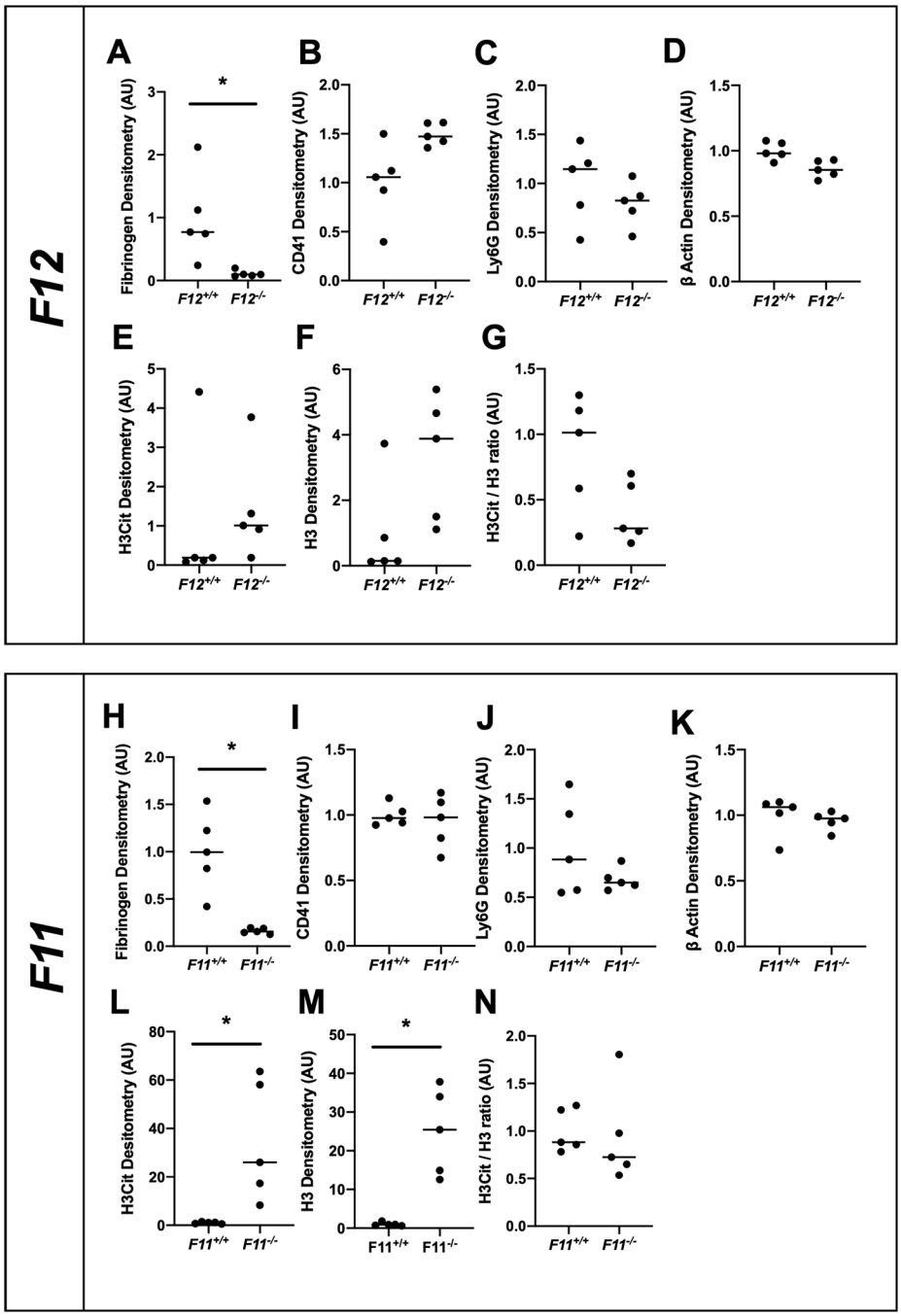

Figure 3: Composition of thrombi formed using the IVC stasis is *F12*$^{+/+}$ mice compared with *F12*$^{-/-}$ mice and *F11*$^{+/+}$ mice compared with *F11*$^{-/-}$ mice

Thrombus composition was assessed in thrombi from *F12*$^{-/-}$ and *F11*$^{-/-}$ mice formed using the IVC stasis model of thrombosis by western blotting of total soluble protein lysates and compared to respective wild-type littermate controls. Densitometric analysis of immunoblots for (A,H) fibrin(ogen), (B,I) CD41, (C, J) Ly6G, (D,K) β actin, (E,L) citrullinated histone H3 and (F,M) total histone H3 for *F12*$^{-/-}$, *F11*$^{-/-}$ mice and wildtype littermate controls. (G,N) The ratio of H3Cit to total H3 was also calculated. *P<0.01 Mann-Whitney U test. Data represented as individual values plus the median.

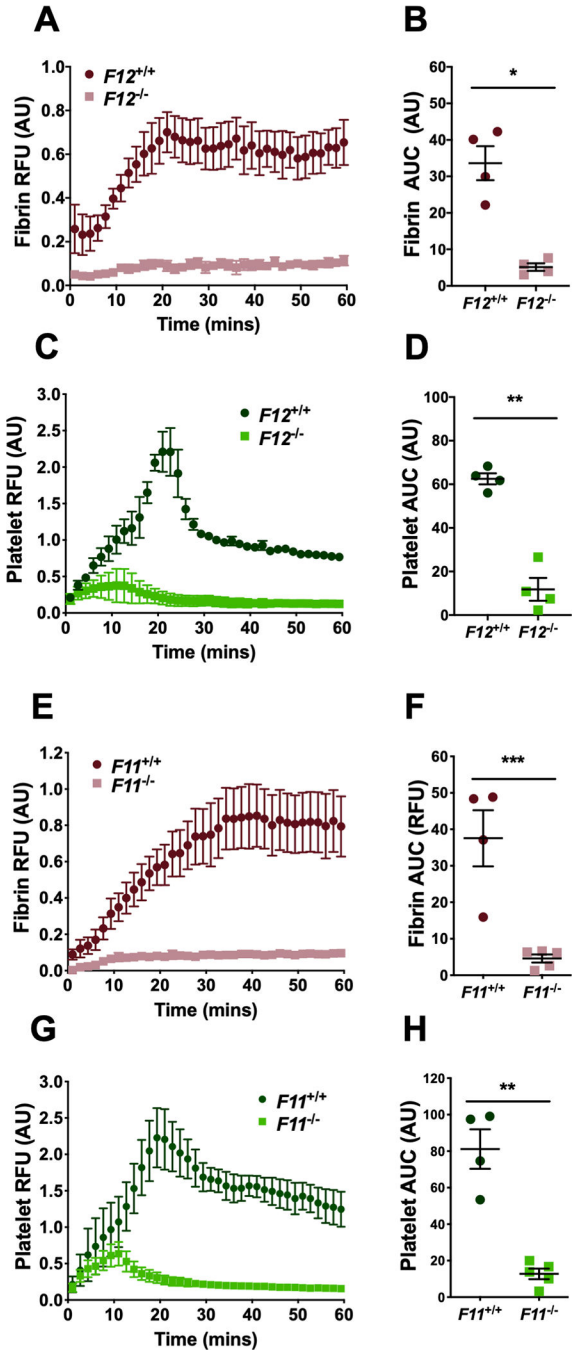

Figure 4: Effect of FXII or FXI deficiency on venous thrombus formation in the mouse femoral vein electrolytic model of thrombosis

Thrombus formation in *F12*$^{-/-}$ and *F12*$^{+/+}$ controls was assessed using the femoral vein electrolytic injury model (n=4 per group). (A) A marked reduction in temporal accumulation of fibrin was observed. (B) Area under the curve measurements demonstrated a significant decrease in total fibrin accumulation at the site of injury in *F12*$^{-/-}$ mice compared to *F12*$^{+/+}$ controls. (C) Similarly, a marked reduction in temporal platelet accumulation was observed in *F12*$^{-/-}$ compared to *F12*$^{+/+}$ controls. (D) Area under the curve measurements demonstrated a significant decrease in total platelet accumulation at the site of injury in

F12$^{-/-}$ mice compared to *F12*$^{+/+}$ controls. Thrombus formation in *F11*$^{-/-}$ and *F11*$^{+/+}$ controls was assessed using the femoral vein electrolytic injury model (n=4–5 per group). (E) A marked reduction in temporal fibrin accumulation was evident in *F11*$^{-/-}$ mice compared to *F11*$^{+/+}$ controls. (F) Area under the curve measurement demonstrated a significant reduction in total fibrin accumulation. (G) A marked reduction in platelet accumulation was also observed in *F11*$^{-/-}$ mice compared to *F11*$^{+/+}$ controls. (H) Area under the curve measurements revealed a significant reduction in total platelet accumulation in *F11*$^{-/-}$ mice compared to *F11*$^{+/+}$ controls. * P<0.001, **P<0.0001, ***P<0.01 Student's t-test. Data represented at mean ± SEM.

Table 1:

Comparative effects of FXII and FXI deficiency in mouse venous thrombosis models

Approach	Model	Phenotype	Ref
ASO	St Thomas'	Targeting FXII and FXI with high level knockdown equally protective	[18]
KO	IVC stenosis	FXII deficiency, but not FXI deficiency, protective	[19]
siRNA	FVEI	Targeting FXII more protective than FXI for intermediate level knockdown	[61]
KO	IVC stenosis	FXII and FXI deficiency equally protective	Current Study
KO	IVC stasis	FXII and FXI deficiency not protective	Current Study
KO	FVEI	FXII and FXI deficiency equally protective	Current Study

antisense oligonucleotide, ASO; inferior vena cava, IVC; short interfering RNA, siRNA, femoral vein electrolytic injury, FVEI; knockout, KO